Compact all-pass filters in photonic crystals as the building block for high-capacity optical delay lines

Zheng Wang
Department of Applied Physics, Stanford University, Stanford, California 94305, USA

Shanhui Fan
Department of Electrical Engineering, Stanford University, Stanford, California 94305, USA
(Received 7 August 2003; published 31 December 2003)

Optical all-pass filters, which generate strong on-resonance optical delay while maintaining a unity transmission coefficient throughout the entire resonant bandwidth, are of great importance for constructing delay lines in optical buffer applications. We provide an analysis of optical delay lines based upon cascading multiple stages of all-pass filter structures. We show that the maximum capacity of such delay lines is determined primarily by the dimensions of each stage. Motivated by this analysis, we describe compact optical all-pass filters in two-dimensional photonic crystals. The accidental degeneracy of the cavity modes introduces a strong group delay and dispersion while maintaining total transmission.

DOI: 10.1103/PhysRevE.68.066616 PACS number(s): 42.70.Qs

Optical all-pass filters are resonant devices that produce strong on-resonance phase variation with respect to the wavelength, while maintaining unity reflectance or transmission over the entire resonance frequency bandwidth. Such filters can generate large group delay and dispersion, and have been used in optical delay lines where multiple stages of all-pass filters are cascaded [1] (Fig. 1). In an optical delay line structure, the unity amplitude response of an all-pass filter is critically important, as it eliminates multiple reflection and interference between the stages. Previously, all-pass filters have been implemented using side-coupled ring resonators [2], optical thin-film filters [3], or Gires-Tournois interferometers [1]. In all these implementations, the size of the device is limited by either intrinsic radiation or diffraction losses.

In this paper, we present an analysis of the capacity of an optical delay line based upon multiple stages of all-pass filters. We show that the capacity of such a delay line is intrinsically limited by the physical dimensions of each stage. Hence it is of critical importance to reduce the footprint of the filter structure. This analysis provides a strong motivation for our implementation of all-pass filter concepts in photonic crystals, since a photonic crystal resonator possesses the smallest footprint achievable using transparent dielectric materials.

We consider the capacity of the general optical delay line structure shown in Fig. 1. The capacity is defined as the total number of pulses that the structure can accommodate without significant spatial overlap between different pulses. For a given spectral bandwidth δf, as determined by the bit rate of the signal, the shortest pulse has a Fourier-transform limited temporal width of approximately $1/\delta f$. The spatial dimension l of such a pulse within the delay line is therefore

$$l = \nu_g \tau = \frac{\nu_g}{\delta f} = \frac{2\pi\nu_g}{\delta\omega}, \qquad (1)$$

where ν_g is the group velocity at the carrier frequency. Hence the maximum total number of pulses that a delay line can accommodate is

$$N = \frac{L}{l} = \int_{\delta\omega} \frac{L}{\frac{d\omega}{dk}} \frac{d\omega}{2\pi} = \int_{\delta\omega} \frac{d\phi}{2\pi} \qquad (2)$$

and is related to the total phase shift ϕ across the entire structure over the signal bandwidth. Since each optical resonance within the bandwidth generates a 2π phase shift [4], the number of pulses that can fit into the delay line (i.e., total number of bits under digital modulation) is determined by the total number of the resonances within the signal bandwidth. Thus the capacity of an optical buffer is in fact limited by the number of resonance that one could fit within the physical length of the delay line.

From the argument presented above, to design a high capacity and compact optical delay line based upon optical resonators, it is sufficient to have the entire resonant linewidth of each resonator fall within the signal bandwidth. Increasing the quality factor of a single resonance beyond such a requirement no longer enhances the capacity of the delay line. The maximal capacity of the delay line is limited solely by the physical dimension of the resonator. In addition, cascading multiple stages of resonators has been shown to be beneficial in reducing the group delay ripples [1]. From these considerations, reducing the dimension of the resonator is of critical importance.

We therefore seek to develop all-pass filter structures based on photonic crystal resonators, as such a resonator

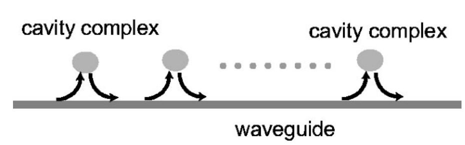

FIG. 1. A multistage all-pass filter consisting of a waveguide and side-coupled resonators. Each stage generates a strong on-resonance optical delay while maintaining unity transmission throughout the entire resonance bandwidth. The aggregate delay of the entire structure is the sum of the delay of each stage.

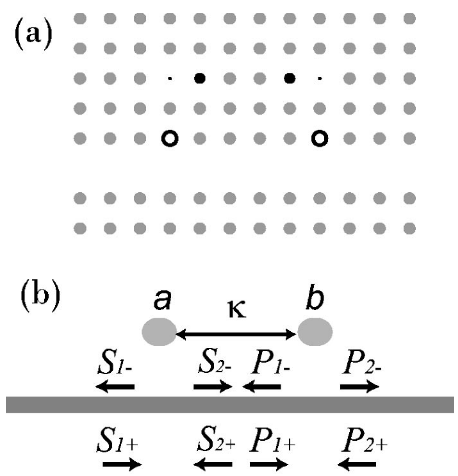

FIG. 2. (a) Schematic of a first order all-pass filter in a two-dimensional photonic crystal. The crystal consists of a square lattice of dielectric rods ($\varepsilon=11.56$) of radius $0.2a$ (gray dots) in air (where a is the lattice constant). The filter consists of a waveguide side-coupled to two single mode cavities, as marked by small dark dots ($\varepsilon=4.2, r=0.05a$). The dielectric constants and the radii of the rods represented by the dark dots ($\varepsilon=13.6, r=0.18a$) and the black circles ($\varepsilon=7.6, r=0.23a$) are chosen to balance the direct and the indirect coupling. (b) Schematic of the theoretical model that describes all relevant coupling mechanisms between two side-coupled resonators and the waveguide.

possesses the smallest modal volume for a given index contrast [5]. Unlike microring resonators, however, most of the photonic crystal resonators support standing-wave modes. A different set of mechanisms in creating all-pass responses is therefore required. Previously, it has been theoretically proposed that either an add/drop filter [6] or an all-pass filter [7] structure can be created by enforcing an accidental degeneracy between two standing-wave cavity modes with opposite mirror symmetry. A study on all-pass filters in photonic crystal structures, however, has never been attempted before. In this paper, we specifically study two first-order optical all-pass filter structures consisting of a waveguide and side-coupled cavities in a two-dimensional photonic crystal. The first photonic crystal structure, as shown in Fig. 2(a), is comprised of a square lattice of high-index dielectric rods with radius $0.2a$ and a dielectric constant of 11.56, where a is the lattice constant. The waveguide is created by removing a single row of dielectric rods in the lattice, and the two cavities are created by reducing the radius of two defect rods. Each cavity supports a localized singly degenerate monopole mode for the TM modes, which has the electric field component parallel to the cylinders [8]. The two cavity modes are evanescently coupled to each other. They are also coupled to the waveguide through the photonic crystal.

Analytically, the response function of such a filter system can be modeled with temporal coupled mode theory [9].

$$
\begin{aligned}
\frac{da}{dt} &= \left(j\omega_0-\frac{1}{\tau}\right)a + j\sqrt{\frac{1}{\tau}}S_{1+} + j\sqrt{\frac{1}{\tau}}e^{-j\phi}P_{2+} + \left(j\kappa-\frac{e^{-j\phi}}{\tau}\right)b,\\
\frac{db}{dt} &= \left(j\omega_0-\frac{1}{\tau}\right)b + j\sqrt{\frac{1}{\tau}}e^{-j\phi}S_{1+} + j\sqrt{\frac{1}{\tau}}P_{2+} + \left(j\kappa-\frac{e^{-j\phi}}{\tau}\right)a,\\
S_{1-} &= e^{-j\phi}P_{2+} + j\sqrt{\frac{1}{\tau}}a + j\sqrt{\frac{1}{\tau}}e^{-j\phi}b,\\
P_{2-} &= e^{-j\phi}S_{1+} + j\sqrt{\frac{1}{+\tau}}e^{-j\phi}a + j\sqrt{\frac{1}{\tau}}b,
\end{aligned}
\tag{3}
$$

where a and b are the amplitudes of the resonant modes in each cavity; $S_{1,2\pm}$, $P_{1,2\pm}$ are the amplitudes of the waveguide modes in various sections of the waveguides as indicated in Fig. 2(b); ϕ represents the phase shift incurred as the waveguide mode travels from cavity a to b; ω_0 is the resonance frequency; τ is the decay rate of the cavity mode due to the coupling to the waveguide, and κ is the mutual coupling coefficient which describes a direct evanescent tunneling process between the resonators, as illustrated in Fig. 2(b). Although the mutual coupling tends to break the degeneracy of the resonances, an indirect coupling, which consists of the resonant amplitude of one cavity decaying into the waveguide, propagating along the waveguide, and coupling into the other cavity, can be designed to cancel the frequency splitting and restore the degeneracy, if the following conditions

$$
\phi=\left(2n+\frac{1}{2}\right)\pi,\ n \text{ as an integer number}
\quad\text{and}\quad \kappa=-\frac{1}{\tau}
\tag{4}
$$

are satisfied [6]. Under this condition, the compound cavity modes can be decomposed as a forward decaying mode F and a backward decaying mode B, where

$$
F=\frac{1}{\sqrt{2}}b-j\frac{1}{\sqrt{2}}a,\qquad
B=\frac{1}{\sqrt{2}}a-j\frac{1}{\sqrt{2}}b.
\tag{5}
$$

Equation (3) can then be simplified as

$$
\frac{dF}{dt}=\left(j\omega_0-\frac{1}{\tau}\right)F+\sqrt{\frac{2}{\tau}}S_{1+},\qquad
P_{2-}=-jS_{1+}+j\sqrt{\frac{2}{\tau}}F,
\tag{6}
$$

where the forward decaying mode F couples only with the forward traveling guided mode amplitudes S_{1+} and P_{2-}. Thus the forward traveling wave is completely decoupled from the backward traveling wave and complete transmission is achieved both on resonance and off resonance. From

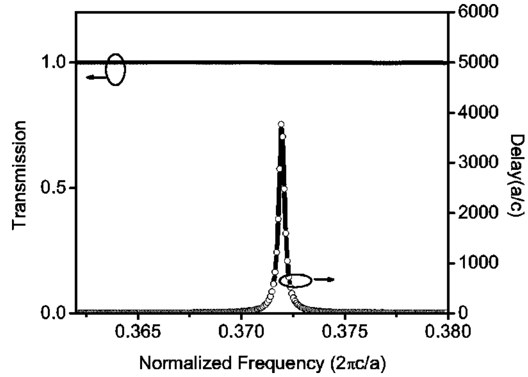

FIG. 3. Transmission and group delay spectrum for the photonic crystal structure shown in Fig. 2(a), as calculated by FDTD simulations.

the steady state solution of Eq. (6), the transmission coefficient for an incident wave S_{1+} at an angular frequency ω can be derived as

$$T=-j\frac{j(\omega-\omega_0)-\dfrac{1}{\tau}}{j(\omega-\omega_0)+\dfrac{1}{\tau}}. \tag{7}$$

The structure behaves as an ideal first-order all-pass filter.

In the photonic crystal structure as shown in Fig. 2, we accomplish the condition as described in Eq. (4) by modifying four specific rods in the photonic crystal [black dots and

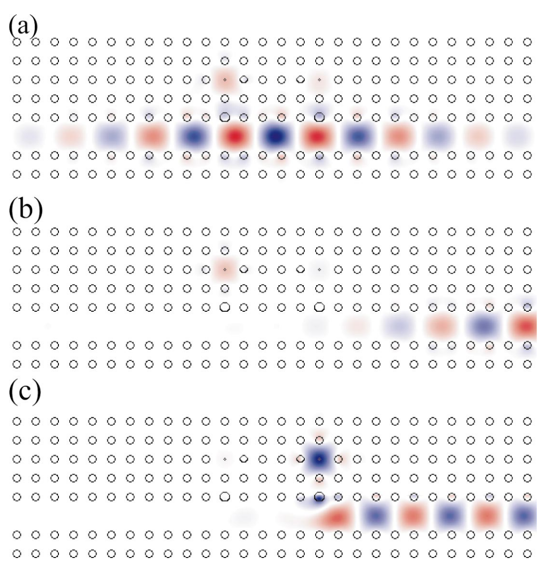

FIG. 4. (Color) Electrical field patterns as a pulse propagates through the photonic crystal structure shown in Fig. 2(a). The pulse has a center frequency at 0.372 c/a, which coincides with the resonant frequency of the cavities, and a temporal width of 2.69 (a/c) that is much shorter than the cavity lifetime. Red and blue represent large positive or negative fields, respectively. The black circles indicate the position of the rods. Shown here are the field patterns when (a): the initial pulse is interacting with the cavities; and (b) and (c): after the initial pulse has passed through the cavities.

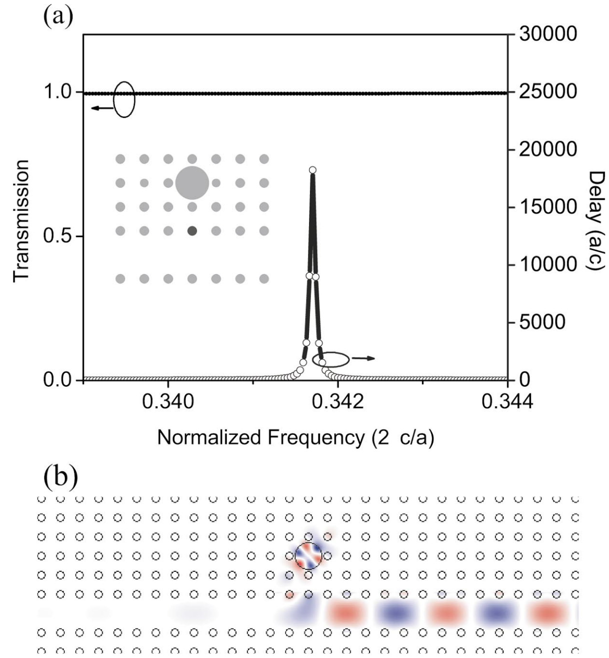

FIG. 5. (Color) (a) Transmission and group delay spectrum for a single-cavity first order all-pass filter in a two-dimensional photonic crystal calculated by FDTD simulations. The inset is a schematic of the structure, which consists of a square lattice of dielectric rods (ε=11.56) of radius 0.2a (gray dots) in air (a is the lattice constant). A cavity is introduced by using a dielectric rod with a radius of 0.7a, which supports two doubly degenerate hexapole modes. The rod, marked by a black dot, has ε=9.4 that is chosen to restore the dependency of the two modes. (b) An electrical field pattern after a pulse, identical to that in Fig. 4, propagates through the all-pass filter.

circles in Fig. 2(a)], and by choosing the resonant frequency such that $\phi=1.25\pi$. To demonstrate the all-pass filter characteristics numerically, we perform a two-dimensional finite difference time domain (FDTD) simulation. The system is excited with a temporal Gaussian source located on the left end of the waveguide. The waveguides are terminated with an absorbing boundary condition specifically designed to suppress reflection from the truncation of a photonic crystal waveguide [10]. The transmission and delay spectra of the system are obtained by performing a discrete Fourier transform for the time-varying field on the right end of the waveguide, and by normalizing with respect to spectra obtained for the waveguide only. The resonators indeed introduce a strong group delay at a frequency of 0.372 (c/a) with a quality factor $Q=1135$ and a maximum delay at 3764(a/c), and the transmission exceeds 99.9% throughout the entire frequency bandwidth (Fig. 3).

The dynamic behavior of the all-pass filter can be exhibited by analyzing the electric field patterns as a pulse propagates through the structure (Fig. 4). A temporal Gaussian pulse is excited at the left end of the waveguide, with a pulse width of 2.69 (a/c) that is far smaller than the cavity lifetime. The pulse travels along the waveguide and excites the cavity mode [Fig. 4(a)]. After the initial pulse has propagated through the resonator, the energy in the resonator continues to slowly decay into the waveguide structure only in the forward direction, while the two resonators oscillate 90° out of phase [Figs. 4(b) and 4(c)]. Such a unidirectional decay indicates that only the forward decaying cavity mode is excited, in consistency with the coupled mode theory presented above for the all-pass filter response.

Instead of using two single-mode cavities, we can further reduce the footprint of the all-pass filter structure by using a single cavity that supports two doubly degenerate states with opposite symmetries [Fig. 5(a) inset]. Increasing the radius of a single rod from $0.2a$ to $0.7a$ creates two degenerate hexapole modes [8]. The degeneracy, however, is broken in the presence of the waveguide, resulting in the decaying constant of the even mode being an order of magnitude greater than that of the odd mode. To restore the degeneracy, we alter the dielectric constant of a rod on the mirror plane between the cavity and the waveguide. The resulting simulated spectra are shown in Fig. 5(a). The structure generates a strong group delay at $0.3417\,(c/a)$ with a quality factor $Q=5446$ and a maximum delay at $18\,240\,(a/c)$, and the transmission exceeds 99.4% throughout the entire frequency bandwidth. Such all-pass characteristics can again be visualized by the unidirectional decay of the cavity mode that is excited by a pulse in the waveguide [Fig. 5(b)]. This structure represents the smallest all-pass filter structure ever proposed. The minimal spacing between stages along the waveguide can be as small as $3a$ (or approximately 1.55 μm when the operating vacuum wavelength is 1.55 μm) when adjacent stages are placed on opposite sides of the waveguide.

As final remarks, we note that the scaling relations, as presented here for optical delay lines, also apply in other applications of cascaded all-pass filter structures, including, for example, the syntheses of arbitrary infinite impulse response filters [11] and on-chip soliton generation [12]. In all these cases, reducing the size of the resonators should result in performance improvement, and thus implementation using a photonic crystal could be beneficial. Also, it has been demonstrated that two-dimensional results can in principle be realized in realistic three-dimensional photonic crystal structures [13]. Thus a high capacity optical delay line can in principle be created based on this all-pass filter design.

This work is supported in part by the NSF under Contract No. ECS-0200445. The authors acknowledge stimulating discussions with D. A. B. Miller.

[1] G. Lenz, B. J. Eggleton, C. K. Madsen, and R. E. Slusher, IEEE J. Quantum Electron. **37**, 525 (2001).
[2] B. E. Little, S. T. Chu, H. A. Haus, J. Foresi, and J.-P. Laine, J. Lightwave Technol. **15**, 998 (1997).
[3] M. Jablonski, Y. Takushima, K. Kikuchi, Y. Tanaka, K. Furuki, K. Sato, and N. Higashi, Electron. Lett. **36**, 1139 (2000).
[4] A. V. Oppenheim, A. S. Willsky, and S. H. Nawab, *Signals and Systems* (Prentice Hall, Upper Saddle River, NJ, 1997).
[5] R. Coccioli, M. Boroditsky, K. W. Kim, Y. Rahmat-Samii, and E. Yablonovitch, IEEE Proc.: Optoelectron. **145**, 391 (1998).
[6] S. Fan, P. R. Villeneuve, J. D. Joannopoulos, and H. A. Haus, Phys. Rev. Lett. **80**, 960 (1998).
[7] Y. Xu, Y. Li, R. K. Lee, and A. Yariv, Phys. Rev. E **62**, 7389 (2000).
[8] P. R. Villeneuve, S. Fan, and J. D. Joannopoulos, Phys. Rev. B **54**, 7837 (1996).
[9] C. Manolatou, M. J. Khan, S. Fan, P. R. Villeneuve, H. A. Haus, and J. D. Joannopoulos, IEEE J. Quantum Electron. **35**, 1322 (1999).
[10] M. Koshiba, Y. Tsuji, and S. Sasaki, IEEE Microwave Wirel. Compon. Lett. **11**, 152 (2001).
[11] C. K. Madsen, J. Lightwave Technol. **18**, 860 (2000).
[12] J. E. Heebner, R. W. Boyd, and Q-Han Park, Phys. Rev. E **65**, 036619 (2002).
[13] M. L. Povinelli, S. G. Johnson, S. Fan, and J. D. Joannopoulos, Phys. Rev. B **64**, 075313 (2001).